Institute of Paper Science and Technology
Atlanta, Georgia

IPST TECHNICAL PAPER SERIES

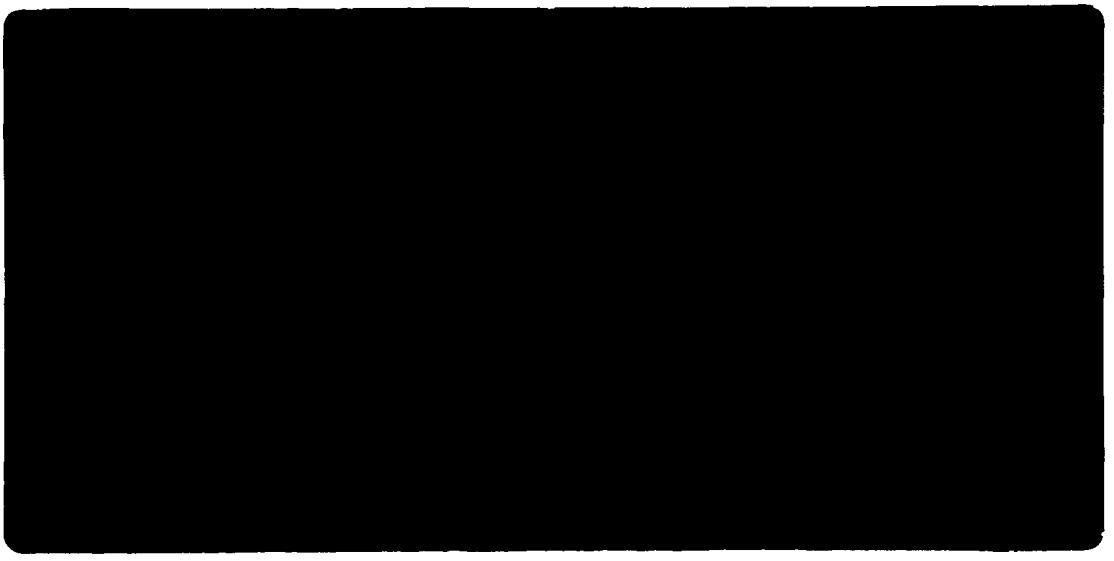

NUMBER 440

ON THE MECHANISM OF CORROSION OF COMPOSITE TUBES AT PORTS IN KRAFT RECOVERY BOILERS

J.A. COLWELL

MAY 1992

On the Mechanism of Corrosion of Composite Tubes at Ports in Kraft Recovery Boilers

J.A. Colwell

Submitted to
7th International Symposium on Corrosion in the Pulp and Paper Industry

ON THE MECHANISM OF CORROSION OF COMPOSITE TUBES AT PORTS IN KRAFT RECOVERY BOILERS

J. A. Colwell
Institute of Paper Science and Technology
575 14th Street, N.W.
Atlanta, GA 30318

ABSTRACT

The relatively rapid wastage of the stainless steel outer layer of composite waterwall tubes at air ports of Kraft recovery boilers has been observed and investigated for several years. The problem is particularly troublesome because it potentially negates the reason for using these tubes in the first place. The rationale for constructing the lower furnace with stainless clad tubes is to avoid the problem of excessive sulfidation of carbon steel tubes as boiler pressures have increased. Thus, the rapid corrosion of the stainless steel may allow the carbon steel to be exposed to a potentially corrosive environment. Most researchers believe that the presence of molten NaOH-based salts cause rapid wastage of the stainless steel. This paper describes a proposed mechanism for corrosion at air ports based on previous work on hot corrosion in gas turbines by molten sodium sulfate. Limited laboratory experimentation supports such a mechanism when applied to molten hydroxide salts. Central to this mechanism is the concept of oxide solubilty as a function of melt basicity.

INTRODUCTION

The problem of corrosion at air ports in recovery boilers using composite (stainless clad steel) tubes is well-documented (1,2). While most of the attention has been focused on air ports, similar corrosive attack has also been observed at other locations such as inspection ports. The corrosion of the stainless steel outer layer is extremely rapid in some cases (up to 150 mpy) and continues until the stainless steel is completely consumed in these localized areas. Usually, once the carbon steel part of the composite tube is exposed, the corrosion rate of the carbon steel decreases to less than 10 mpy. There is concern that if the environmental conditions should change near the area where the stainless steel is depleted, rapid sulfidation of the carbon steel inner tube may occur. However, in the highly oxidizing area of the air port, reducing conditions would not be expected. But, in any case, it is desirable to understand the corrosion mechanism in these areas so that life of the waterwall tubes can be estimated with some degree of accuracy. Currently, the mechanism of air port corrosion is not completely understood, but it has been suggested that condensation

of NaOH is responsible (3). Several different mechanisms have been postulated, including galvanic effects between the stainless steel outer layer and the carbon steel inner layer.

In gas turbines, especially those operated over seawater, a phenomenon was discovered in the late 1960's by which rapid corrosion of Ni-base superalloys was caused by continued sulfidation/oxidation of the alloy (4,5). The mechanism has been studied for some time and it is generally agreed that the presence of a thin molten Na_2SO_4 salt film initiates and propagates the attack (6). The same effect is also observed in molten sodium carbonate fuel cells with Ni (7). For Kraft recovery boilers, because the corrosion of the stainless steel at air ports may also be initiated by a molten salt, i.e., NaOH, a similar mechanism may be responsible.

REVIEW OF HOT CORROSION BY MOLTEN SODIUM SULFATE

Thermodynamics and Salt Chemistry

Much of the hot corrosion research on molten sulfates has been conducted and reviewed by Rapp and his co-workers (8,9); it will be highlighted here to aid the reader.

Oxyanion melts of alkali nitrates, carbonates, hydroxides and sulfates exhibit an acid-base behavior whereby the acid component is NO_2, CO_2, H_2O, or SO_3, respectively. The basic component can be chosen as the oxide ion or the Na_2O component in all of these cases. Consequently, for molten Na_2SO_4,

$$Na_2SO_4 \rightleftharpoons Na_2O + SO_3$$

where the basic component is Na_2O and the acid component is SO_3. For the pure salt, the specification of either acidity or basicity is sufficient, because of the above equilibrium. For mixed melts, if only a single cation is present, e.g., Na^+, and mixed anions, then basicity is the parameter which is to be chosen to describe the melt. However, when mixed cations are present with a single anion, the acidity parameter is more appropriate.

Phase stability diagrams can be used in describing the thermodynamics of the system; these are completely analogous to the plots pioneered by Pourbaix for aqueous corrosion (10). Plots of electrode potential (oxidizing potential or oxygen activity) vs. basicity ($-\log a_{Na2O}$) are useful in the molten salt case. During the course of development of these diagrams a convention resulted in acidity increasing to the right, opposite to aqueous systems. Figure 1 shows the Na-S-O phase stability diagram at 900 C (9). In addition to delineating the major stable phase fields, the regions of dominance for the minority ionic species are also given. This

allows consistent explanations for chemical and electrochemical reactions using the criterion that spontaneous reactions involve the consumption of unstable species and the formation of stable products for the local conditions.

Oxide Solubilities

From a knowledge of the Na-metal-S-O phase stability diagram, and independent measurements of basicity, and oxygen activity, the solubilities of various oxides have been determined at 1 atm P_{O_2} at 1200 K (11). The phase stability diagrams for Na-Fe-S-O and Na-Cr-S-O are given in Figures 2 and 3, respectively. The corresponding solubility curves are given in Figures 4 and 5. Based on certain assumed soluble ions, the dependence of the solubility of a particular ion on basicity can be compared to the experimental slope of the curve. Agreement between the experimental and theoretical slopes reveals the identity of the soluble ion. The agreement of the experimental data to the theory is remarkable and validates the approach.

Figure 6 represents a compilation of measured solubilities for oxides pertinent to high temperature alloys. The stability of various oxides depends upon the local basicity of the melt. At high basicities, the stabilities of Co and Ni oxides are greater than Cr and Al oxides, but the situation is reversed at much lower basicities.

Fluxing Mechanisms

An early mechanism (12) of hot corrosion suggested that the gradient in the solubility of the protective oxide in the salt film (either as a basic or acidic solute) is negative at the oxide salt interface:

$$\left.\frac{d(\text{oxide solubility})}{dx}\right|_{x=0} < 0$$

Then, from Figure 7, the oxide scale would dissolve to satisfy its saturation concentration at the scale/salt interface. The solute ions would diffuse down the concentration gradient in the salt film and precipitate as nonprotective oxide particles where the oxide solubility is lower.

Figure 8 provides a schematic plot of oxide solubility with the superposition of different basicities at the oxide/salt interface I, and the salt/gas interface II. These conditions set up and maintain continuous hot corrosion according to the model. If the basicity gradient is reversed, then the entire salt film becomes saturated, and hot corrosion stops. This plot is key to

understanding when hot corrosion is expected and when conditions are unfavorable.

The electrochemical model for the hot corrosion of an initially passivated metal is shown in Figure 9. Two cases are considered, one where the concentration of solute transition metal ions is small so that the reduction step occurs at the oxide/salt interface. Consequently, the basicity is high at that interface because of the locally high concentration of oxide ions. The other case occurs when an appreciable concentration of transition metal ions is present, which allows the reduction step to occur at the salt/gas interface, where the basicity would be higher. In either case, acidic or basic solutes will form based on the oxide solubility plot, i.e., the overall basicity. The shift of the reduction reaction to the salt/gas interface should accelerate oxide dissolution because the need for oxidant diffusion through the salt film to the oxide surface would not be required.

APPLICATION TO AIR PORT CORROSION

The application of the above concepts to air port corrosion begins with the molten salt equilibrium reaction, i.e.,

$$2NaOH \rightleftharpoons Na_2O + H_2O$$

The basic component is Na_2O and the acidic component is H_2O. While it is likely that KOH is also present in the NaOH, the initial treatment will consider only the presence of NaOH.

To consider corrosion of composite waterwall tubes (stainless steel outer tube and carbon steel inner tube), the discussion will treat each of the materials independently first. The dissolution of the two oxides which are normally present on the surface, namely Cr_2O_3 and Fe_2O_3, will be used to describe the corrosion of the stainless steel and carbon steel, respectively. We know that the corrosion rate of stainless steel is much more rapid than that of carbon steel. This is observed in service and has been simulated in the laboratory. Differences in corrosion rates of more than an order of magnitude can be observed. Measurements of galvanic currents (13) show that Type 304 stainless steel corrodes preferentially compared to carbon steel, but the magnitude of those currents do not justify the high weight loss of the stainless steel. Consequently, even though galvanic corrosion contributes, it is not the controlling mechanism.

If we begin with the schematic solubility curves of Figure 10, it is assumed that the shape and relative position in NaOH at temperatures just above its melting point are similar to those measured in sodium sulfate at 1200 K (9). The only basicities where the solubility (i.e., corrosion) of Cr (stainless steel)

would be more than that of Fe (carbon steel), is to the left of point 'a'. Thus, corrosion of Cr might be greater than that of Fe in melts where the basicity was greater than 'a'. In fact, because of the differences in the corrosion rates, one would expect that the actual basicity in service would be far from 'a' and be much further to the left on the diagram.

Cr_2O_3 Dissolution

Because the basicity of the melt which causes the chromium oxide solubility to be greater than that for iron oxide (corrosion of stainless steel greater than carbon steel) is to the left of the chromia minimum, it is apparent that chromia dissolves as a basic solute. And, because of the relatively high P_{02} in the air, dissolution is probably as CrO_4^{2-}, by the following reaction:

$$Cr_2O_3 + 2\ O^{2-} + 3/2\ O_2 \rightleftharpoons 2CrO_4^{2-}$$

This is borne out by our laboratory observation that when chromia powder is added to the melt for the Type 304 stainless steel corrosion tests, the corrosion rate decreases and the melt turns yellow, which is the color of chromate. This is a result of the reduced basicity which occurs when Cr_2O_3 is added to the melt.

Figure 11 gives the schematic electrochemical model for the chromia dissolution case. The reduction step is most likely oxygen reduction by diffusion of oxygen through the salt film and arrival at the oxide/salt interface. Thus, the basicity is locally high at that location, and Figure 12 summarizes the local solubilities at both interfaces. Because the solubility is higher at the oxide/salt interface, dissolution will readily occur and oxide precipitation will occur toward the salt/gas interface. Thus, continued hot corrosion should be observed, giving high corrosion rates.

Fe_2O_3 Dissolution

For the dissolution of Fe_2O_3, which is being used to consider the corrosion of carbon steel, two cases need to be considered depending on whether the melt basicity is to the left or right side of the solubility minimum.

Basic Dissolution

In this case the basicity is to the left of the minimum in the solubility curve and the oxide ion reacts with hematite to form the ferrite ion or ferrate ion depending on the oxidizing power of the solution:

$$\text{reducing:} \quad Fe_2O_3 + O^{2-} \rightleftharpoons 2\ FeO_2^-$$

$$\text{oxidizing:} \quad Fe_2O_3 + 3\ O^{2-} \rightleftharpoons 2\ FeO_3^{3-}$$

It is known that $NaFeO_2$ has a very low solubility in NaOH, so the reaction would tend to be slow, but the gradient in solubility would be negative (like previous discussion on chromia) and the tendency would be for the reaction to continue as a hot corrosion reaction.

Acid Dissolution

In this case oxide ions would be generated by the acid dissolution of Fe_2O_3:

$$Fe_2O_3 \rightleftharpoons 2\ Fe^{3+} + 3\ O^{2-}$$

The basicity would again be higher at the oxide/salt interface, but because the overall basicity is on the acid side of the curve, this means this location has a lower solubility. Thus, the solubility gradient is positive, and the reaction would reach some equilibrium where the melt is saturated with the solute and the reaction essentially stops.

Basic Dissolution with Transport of Transition Metal Ions

This case is shown in Figure 13, where the reduction step shifts to the salt/gas interface. At the oxide/salt interface, hematite complexes with the oxide ion to form ferrite ion which diffuses down its concentration gradient. Also, ferric ion is reduced to ferrous ion, causing transport of ferrous ions to the salt/gas interface where they react with oxygen. This causes the reduction of oxygen to oxide ion and the reoxidation of ferrous ions to ferric ions. Thus, the basicity increases at the salt/gas and decreases at the oxide/salt interface (by consumption to form ferrite ions). So, the solubility is higher at the gas/salt interface, and a positive solubility gradient exists, which should limit hot corrosion. Note that in this case diffusion of the oxidant through the salt is not required.

Therefore, there are two mechanisms which would be consistent with the observation of a low corrosion rate for carbon steel. Normal acidic dissolution and basic dissolution with ferrous ion transport are both possible. Our limited laboratory work and field measurements indicate that the corrosion rate of carbon steel is extremely low, so one of these mechanisms is probable.

Corrosion of Alloys

In the recovery boiler both stainless steel and carbon steel are present, rather than pure Cr and Fe, so pure oxides of Cr and Fe will not be present. One important question that needs to be resolved is whether Fe (i.e., carbon steel) has such a low corrosion rate and Type 304 stainless steel is nominally 74 percent Fe, why is the stainless steel completely corroded away leaving no hematite film (or NiO, for that matter) which would protect the remainder of the stainless steel because of its lower solubility.

Acidic dissolution of Fe_2O_3 and NiO (the Fe and Ni from the stainless steel) could be used to explain this phenomenon. The production of oxide ions from the dissolution of both the Fe_2O_3 and the NiO would be consumed by the basic dissolution of Cr_2O_3. This has been demonstrated by Hwang and Rapp in molten sodium sulfate (14). The normally protective film on stainless steel is likely composed of Fe, Ni and Cr cations in close proximity on the M_2O_3 lattice so the dissolution and transfer of oxide ions from the Fe- and Ni-rich locations to the Cr-rich locations near the oxide/salt interface could occur extremely rapidly. Oxygen transport to that interface allows the reduction reaction to oxide ions which adds to the supply generated by the acid dissolution of Fe_2O_3 and NiO. Because of the consumption of the oxide ions by the chromia, the solubility gradient is negative, instead of being positive when dissolution of the individual Fe- and Ni-oxides occur. The salt never becomes saturated in Fe and Ni oxides, so the reaction continues until the stainless steel is consumed.

So, in the case of stainless steel corrosion, the reaction does not stop until the stainless steel is consumed, and then the slower reactions involving Fe_2O_3 only (the carbon steel inner part of the composite tube) take over, and the corrosion essentially stops due to the saturation of solute as a result of the positive solubility gradient. However, if the salt is removed, as would occur during a boiler shut-down, the process would start once again and consume some amount of carbon steel until saturation occurs.

MODEL VALIDATION FROM LABORATORY EXPERIMENTS

To test some of the features of this proposed mechanism, a few experiments were conducted to determine whether the data would support the main points of the theory.

Weight loss corrosion tests on several different materials were

conducted in pure NaOH at 320 C for various times. Alloy wires were placed in an alumina crucible containing the molten NaOH for the specified time. A summary of the weight loss for each is shown in Table 1. The top part of the table covers experiments which were conducted with a cover gas of flowing dry air. From these data, the weight loss of carbon steel remains approximately constant at exposure times between 5 and 168 hours. In contrast, the Type 304 stainless steel continues to lose weight at about the same rate over the same time period. This result is consistent with the model presented here, i.e., chromia dissolution is occurring via a hot corrosion mechanism. Also, the fact that the weight loss of carbon steel remains essentially constant (hematite film presumed) indicates that dissolution is either by the acidic mechanism or the basic dissolution with transition metal ion transport mechanism. Either of these two mechanisms predict that the salt film will eventually become saturated with solute and the reaction will then essentially stop, which is observed when the weight loss becomes constant.

Because the model requires that both oxidation and reduction reactions occur to generate the high rates of corrosion of stainless steel, a set of experiments was conducted to stifle the reduction reaction by limiting oxygen transport to the oxide/salt interface. This was accomplished by changing the cover gas to nitrogen with a very low oxygen content. The corrosion data for this case is shown in the last two entries in Table 1. Note that reducing oxygen had very little effect on the corrosion of carbon steel, as would be predicted, because that reaction is controlled by solute saturation due to its positive solubility gradient. In contrast, note that the corrosion of 304 stainless steel was essentially stopped, even up to 139 hours. Another test was devised to determine if the reaction could be slowed by removing the oxidation step, so pure Cr_2O_3 was used to remove the possibility of the formation of Cr^{3+}. These results are also given in Table 1, and as can be seen, the weight loss is much less than that of the 304 stainless steel. Consequently, the model appears to be valid relative to the oxidation and reduction steps.

Another feature of the model is concerned with the acceleration of corrosion of Cr in a stainless steel because dissolution of Fe- and Ni-oxides supply oxide ions which complex with chromia. An experiment was completed where pure Cr metal was compared to the rate of corrosion of 304 stainless steel. The model would predict that the corrosion of pure Cr would be less than that of stainless steel, and that is what was observed, as given in Table 1. The corrosion rate of pure Cr is still greater than that of Fe, by virtue of the position of the two solubility curves, but is smaller than 304 stainless steel by a factor of about two.

A series of experiments was conducted to examine the effect of basicity when the melt is equilibrated in an air cover gas. The data for the "normal" basicity of the melt is again given for comparison, along with data for corrosion in more basic as well as more acidic melts. The more basic melts were achieved by the

addition of Na_2O_2, and the acidic melts were obtained by equilibration with a large fraction of H_2O vapor in the flowing air cover gas. The data are summarized in Table 2. The corrosion rate of the carbon steel is at a minimum in the normal melt, and it is accelerated when the basicity is made either more acidic or more basic. Thus, the basicity of the normal melt must be near the solubility minimum for Fe_2O_3, with changes to more basic melts causing basic dissolution at a higher rate. Modifications which cause the melt to become more acidic must change the dissolution mechanism to that of an acidic solute. In contrast, the 304 stainless steel data show that the corrosion rate continues to decrease as basicity decreases, so the basicity must remain on the basic side of the Cr_2O_3 minimum.

Thus, the limited number of experiments conducted thus far seem to support the proposed mechanism. Much work remains to be completed to confirm all the details. For example, areas that need attention are determining the effect of melt chemistry on solubilities, and developing a technique for the reliable measure of basicity.

SUMMARY

The corrosion of composite waterwall tubes in the lower furnace of Kraft recovery boilers has been explained on the basis of previous investigations of hot corrosion of gas turbines. In the case of gas turbines, a molten salt of Na_2SO_4 caused rapid attack of Ni-base alloys. In recovery boilers the salt is NaOH, or a eutectic mixture with K, and the stainless steel outer layer of the tube is subjected to the rapid wastage.

The corrosion mechanism of the stainless steel (Fe-Cr-Ni alloy) can be summarized as basic dissolution of Cr_2O_3, with acidic dissolution of Fe_2O_3 and NiO, which promotes the synergistic dissolution of all components in the alloy. Once the stainless steel has dissolved, the model predicts that the remaining carbon steel is not susceptible to the same rapid corrosion rates observed for stainless steel because the solute becomes saturated in the molten salt.

Experiments conducted to determine the effect of melt basicity show that corrosion of stainless steel can be reduced (to about 70 mpy) by decreasing melt basicity, i.e., by increasing water content of the gas above the molten NaOH. However, at the same time, the corrosion of carbon steel is increased to unacceptable levels (about 900 mpy). Consequently, because the corrosion of the carbon steel inner layer is the controlling factor in pressure containment, modifying melt basicity will need to be carefully considered before it is a viable method for corrosion control.

REFERENCES

1. D. A. Wensley, TAPPI Kraft Recovery Operations Seminar Notes, TAPPI Press, pg. 231 (1986).

2. M. A. Lunn, W. B. A. Sharp, J. D. Andrews, H. N. Tran, and D. Barham, 6th International Symposium on Corrosion in the Pulp and Paper Industry, NACE, pg. 151 (1989).

3. T. Odelstam, H. N. Tran, D. W. Reeve, D. Barham, R. Backman, and M. Hupa, TAPPI Engineering Conf., pg. (1987).

4. M. A. DeCrescente and N. S. Bornstein, Corrosion, 24, 127 (1968).

5. J. A. Goebel and F. S. Pettit, Met. Trans., 1, 1943 (1970).

6. N. S. Bornstein and M. A. DeCrescente, Met. Trans., 2, 2875 (1971).

7. M. L. Orfield and D. A. Shores, J. Electrochem. Soc., 135, 1662 (1988).

8. M. Kawakami, K. S. Goto and R. A. Rapp, Trans. Iron and Steel Inst. Japan, 20, 646 (1980).

9. R. A. Rapp, Corrosion, 42, 568 (1986).

10. M. Pourbaix, Atlas of Electrochemical Equilibria, NACE, 1974.

11. C. O. Park, R. W. Geist and R. A. Rapp, in Localized Corrosion; Equilibrium Diagrams, R. Frankenthal, J. Kruger, eds., ECS Symposium Series, Electrochemical Society, Pennington, NJ, p. 228, 1984.

12. R. A. Rapp and K. S. Goto, The Hot Corrosion of Metals by Molten Salts, in Molten Salts, J. Braunstein and J. R. Selman, eds., Electrochemical Society, Pennington, NJ, p. 81, 1981.

13. J. A. Colwell and G. Fonder, proprietary report to IPST member companies, 1991.

14. Y. Hwang and R. A. Rapp, J. Electrochem. Soc. 137, 1276 (1990).

Table 1. Weight-loss of Various Materials in Molten NaOH at 320 C.

		Weight-Loss, mg/cm^2			
Time,hr	Environment	Carbon Steel	304 SS	Pure Cr	Pure Cr_2O_3
5	NaOH (air)	11.6	0.6	-	-
24	NaOH (air)	13.9	7.2	-	-
72	NaOH (air)	13.2	26.2	-	6.2
168	NaOH (air)	15.2	79.5	36.2	-
24	NaOH (N_2)	10.2	0.35	-	-
139	NaOH (N_2)	11.3	0.41	-	-

Table 2. Effect of Basicity Changes on the Corrosion of Carbon Steel and Stainless Steel in NaOH at 320 C for 72 hours

	Weight-loss, mg/cm^2	
Environment	Carbon Steel	304 SS
NaOH + 10%Na_2O_2 (basic)	25.7	43.2
NaOH	13.2	26.2
NaOH + 80%H_2O (acidic)	145.7	10.4

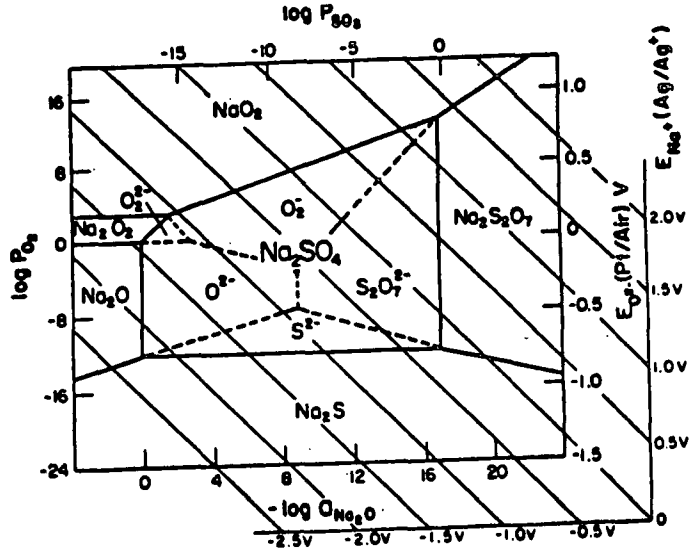

Figure 1. *Na-S-O phase stability diagram for 900 C. After Rapp (9).*

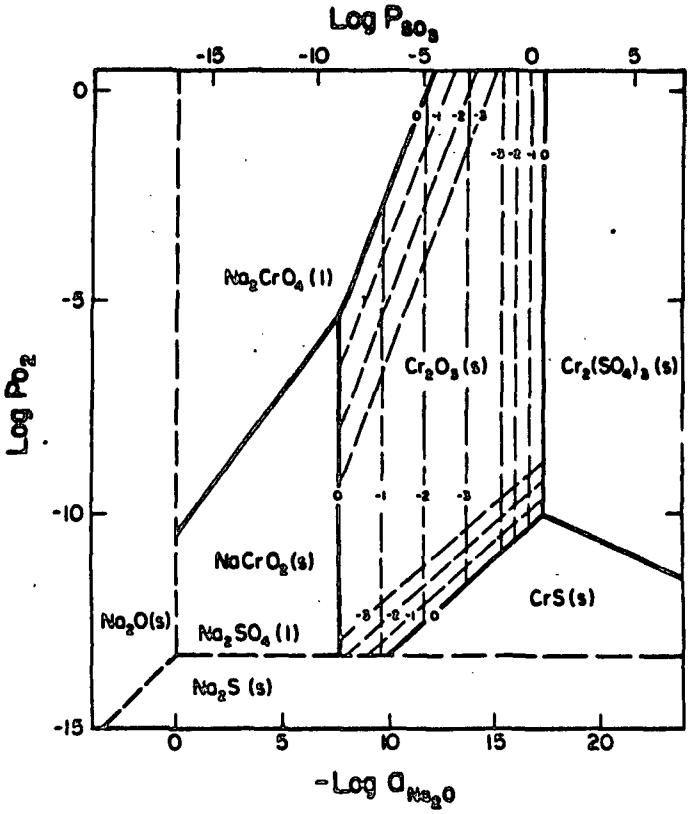

Figure 2. *Na-Cr-S-O phase stability diagram for 1200 K. After Rapp (9).*

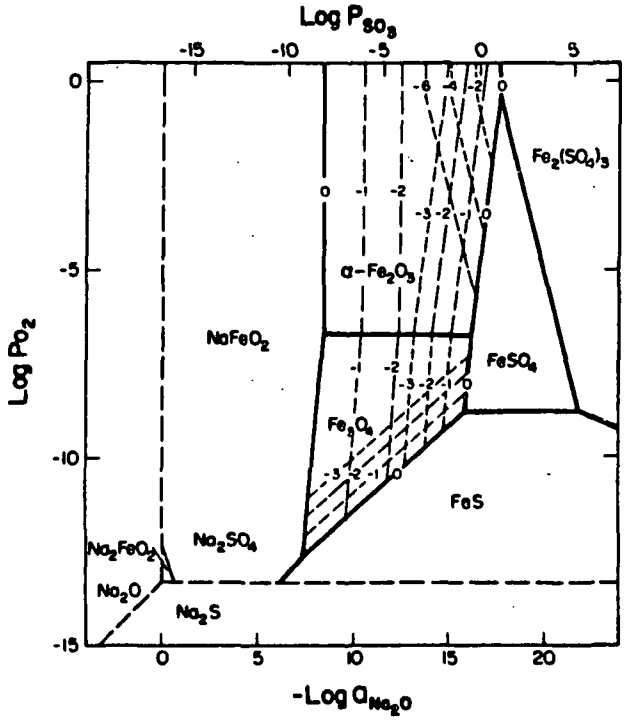

Figure 3. ***Na-Fe-S-O phase stability diagram for 1200 K. After Rapp (9).***

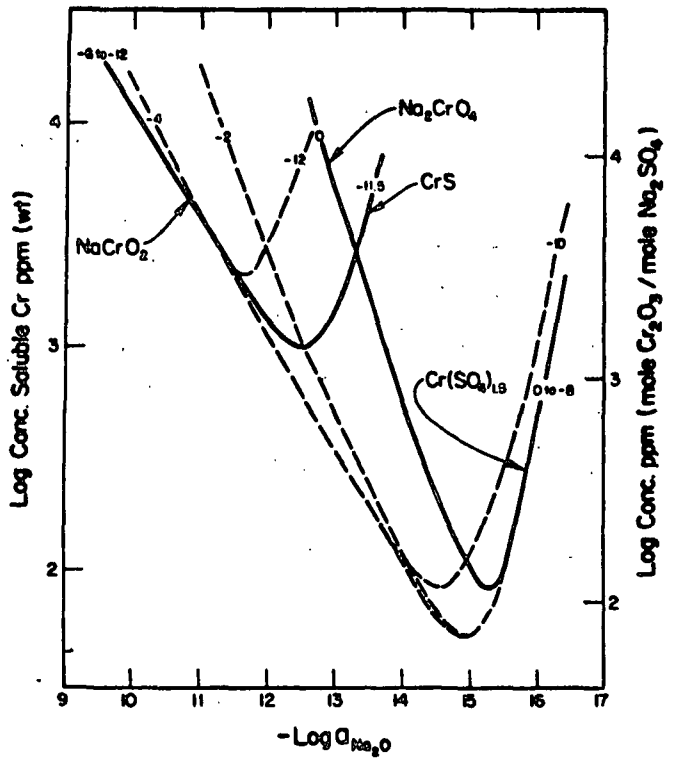

Figure 4. ***Measured and calculated solubilities of Cr_2O_3 in fused Na_2SO_4 at 1200 K for several oxygen activities. After Rapp (9).***

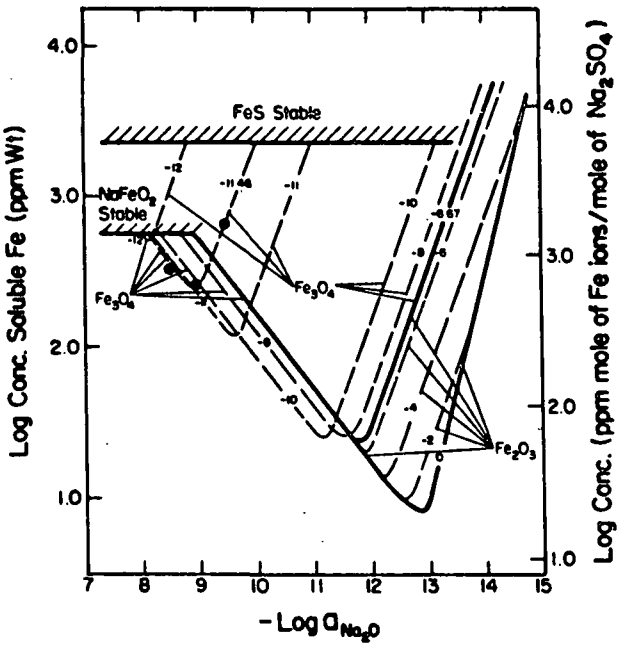

Figure 5. ***Measured and calculated solubilities of α-Fe_2O_3 and Fe_3O_4 in fused Na_2SO_4 at 1200 K for several oxygen activities. After Rapp (9).***

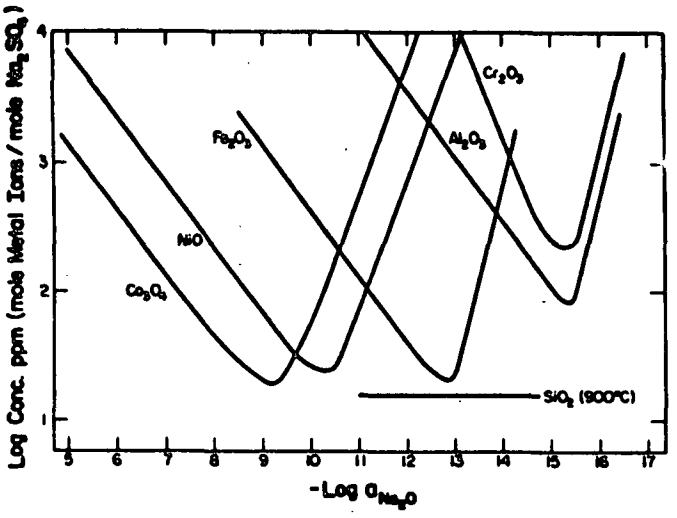

Figure 6. ***Measured oxide solubilities in fused Na_2SO_4 at 1200 K and 1 atm O_2. After Rapp (9).***

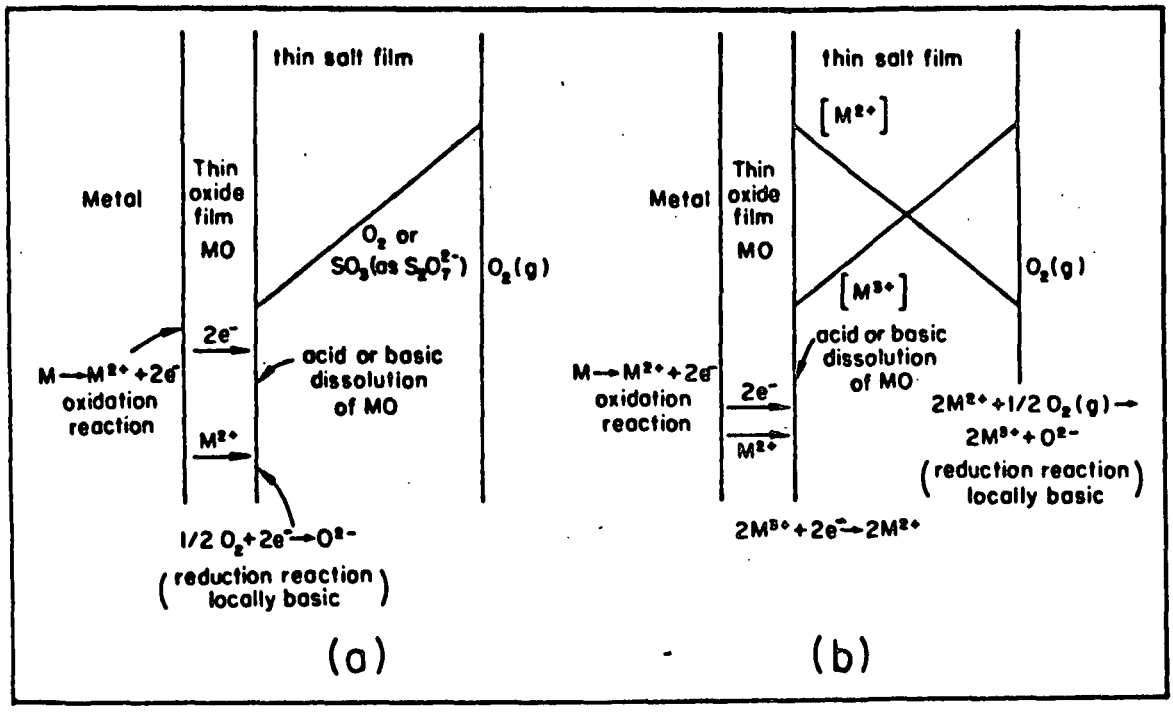

Figure 7. ***Cathodic reduction of SO_3 (as $S_2O_7^{2-}$) or molecular oxygen for (a) a high permeability of SO_3 or O_2 in thin salt film, (b) high concentrations and diffusivities of M^{2+} and M^{3+}, or electronic conduction, in the salt film. After Rapp (9).***

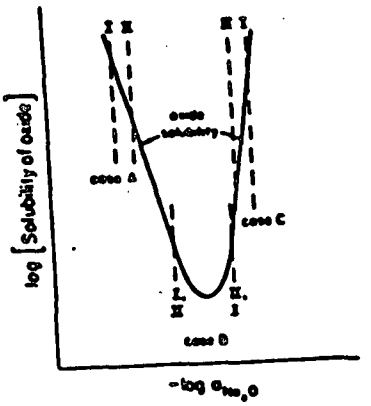

Figure 8. *Cases of Continuous Hot Corrosion of a Pure Metal (I is the oxide/salt interface, and II is the salt/gas interface). After Rapp and Goto (12).*

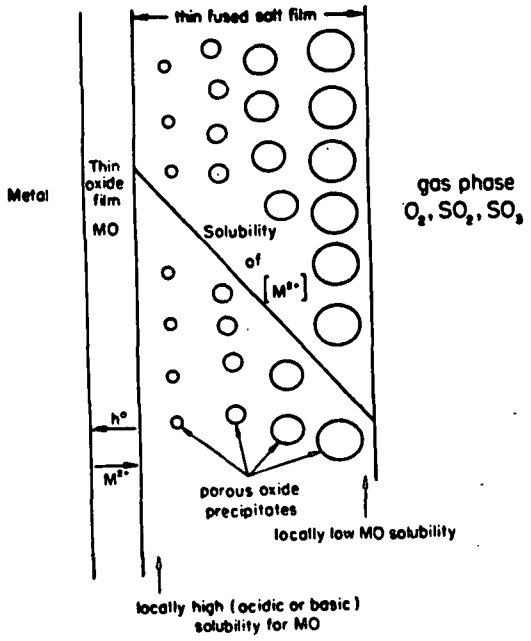

Figure 9. ***Reprecipitation of a porous MO oxide supported by the solubility gradient in a fused salt film. After Rapp and Goto (12).***

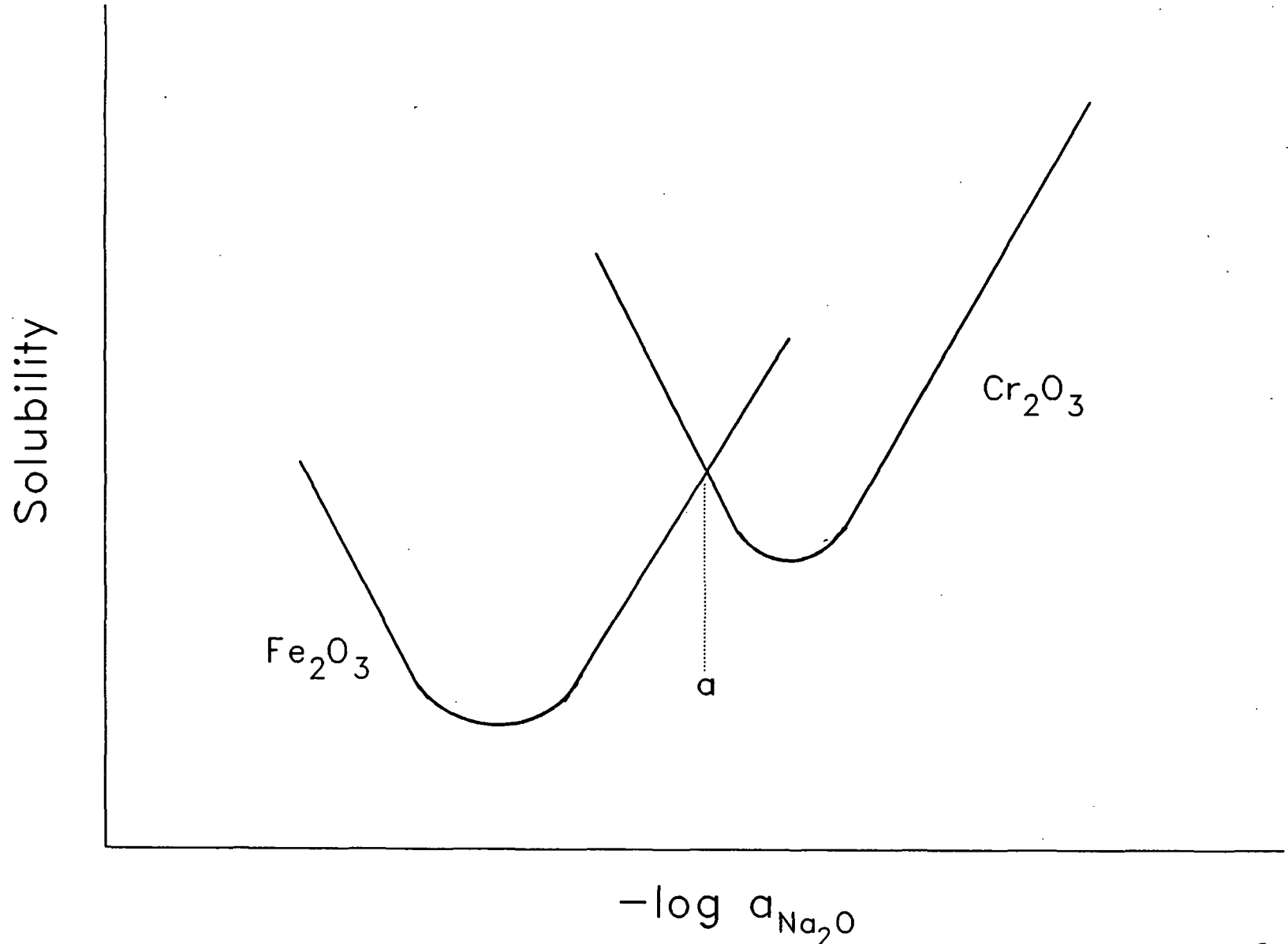

Figure 10. ***Schematic Solubility Curves for Fe_2O_3 and Cr_2O_3. Point "a" indicate basicity where Cr_2O_3 solubility is greater than Fe_2O_3.***

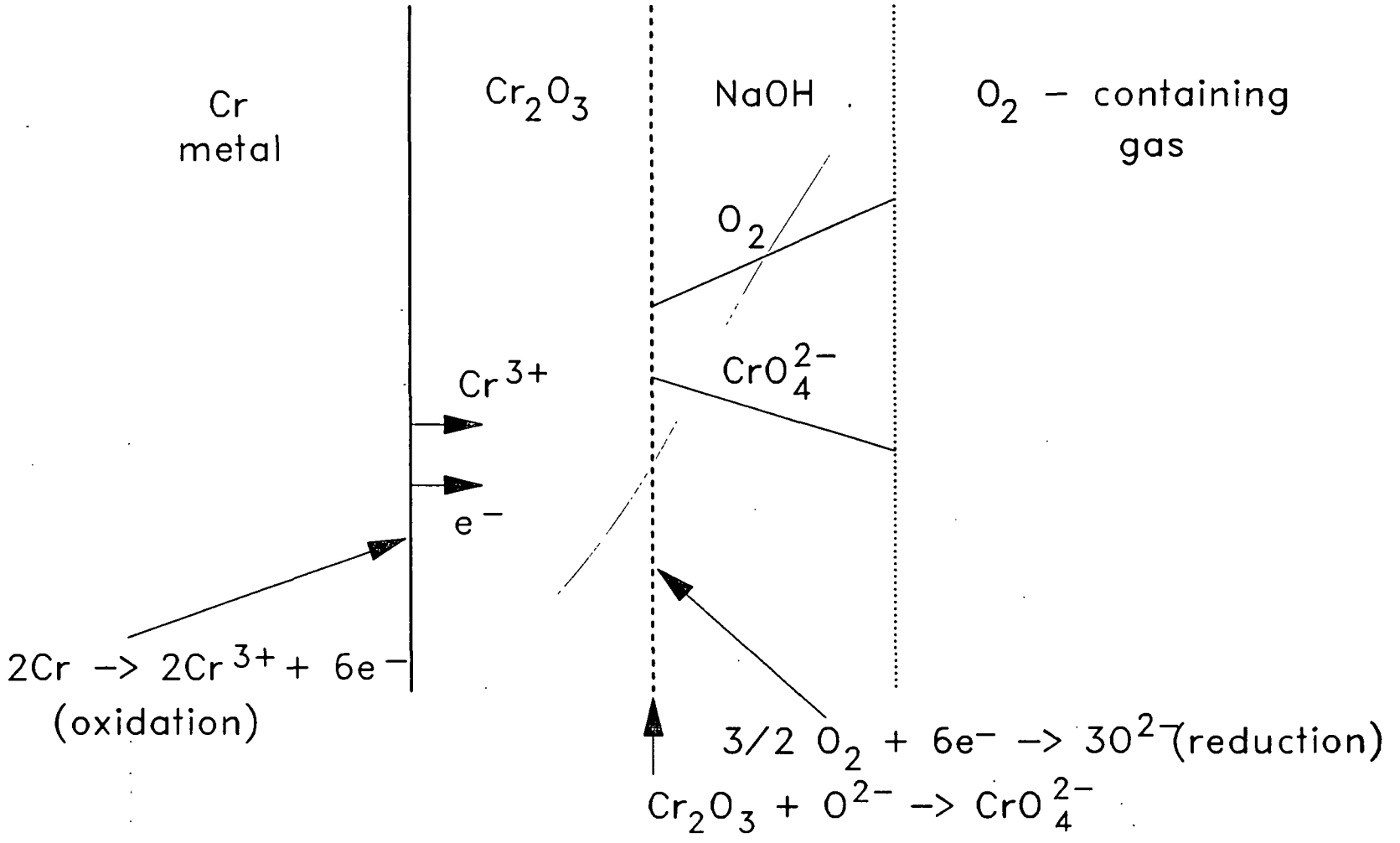

Figure 11. ***Electrochemical Model for the Corrosion of Cr in Molten NaOH in an Oxygen Containing Gas. Negative Solubility Gradient Allows Continuation of Hot Corrosion.***

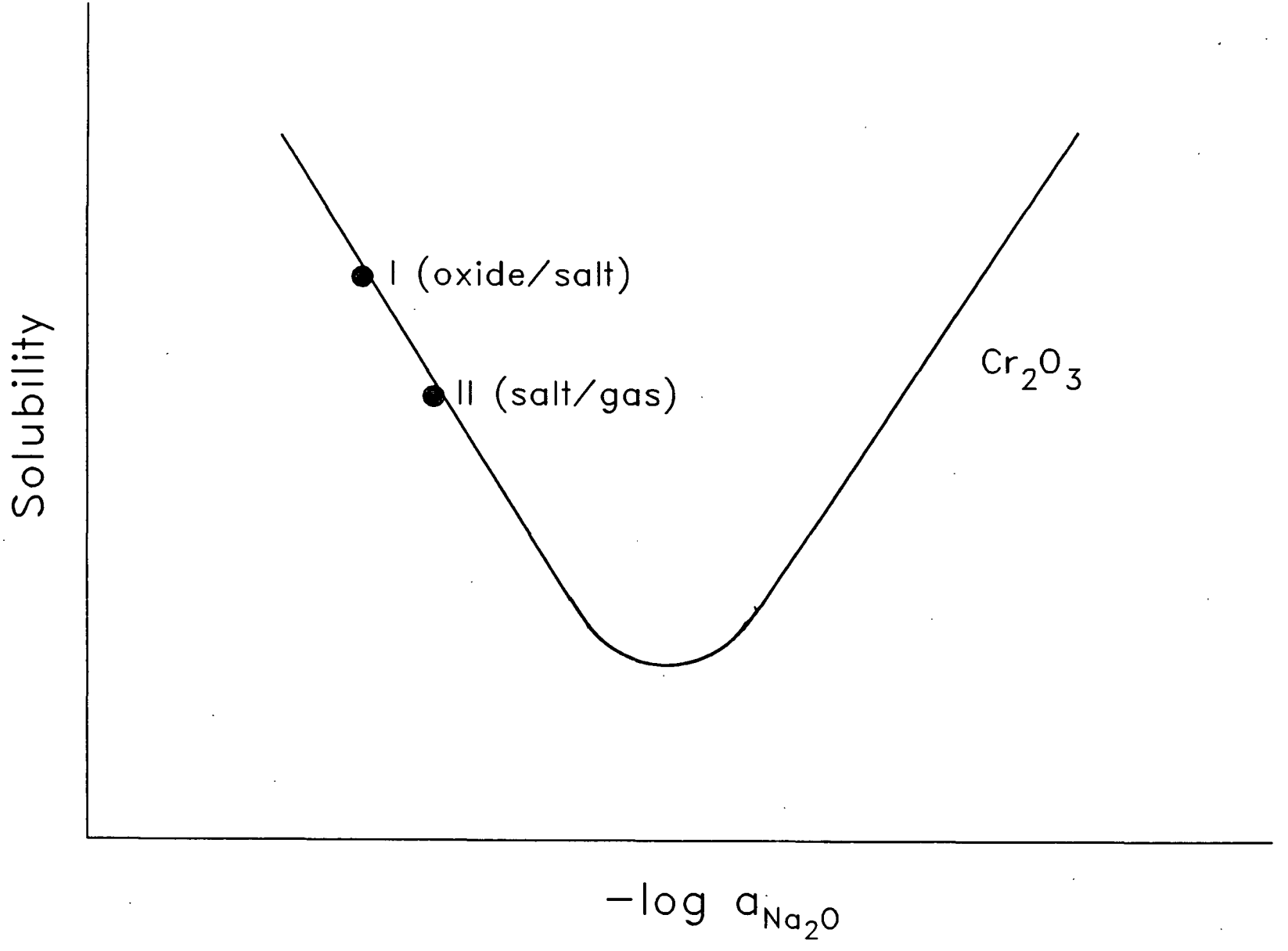

Figure 12. ***Local Solubilities at Oxide/Salt (I) and Salt/Gas (II) Interfaces for Continued Hot Corrosion of CR in NaOH.***

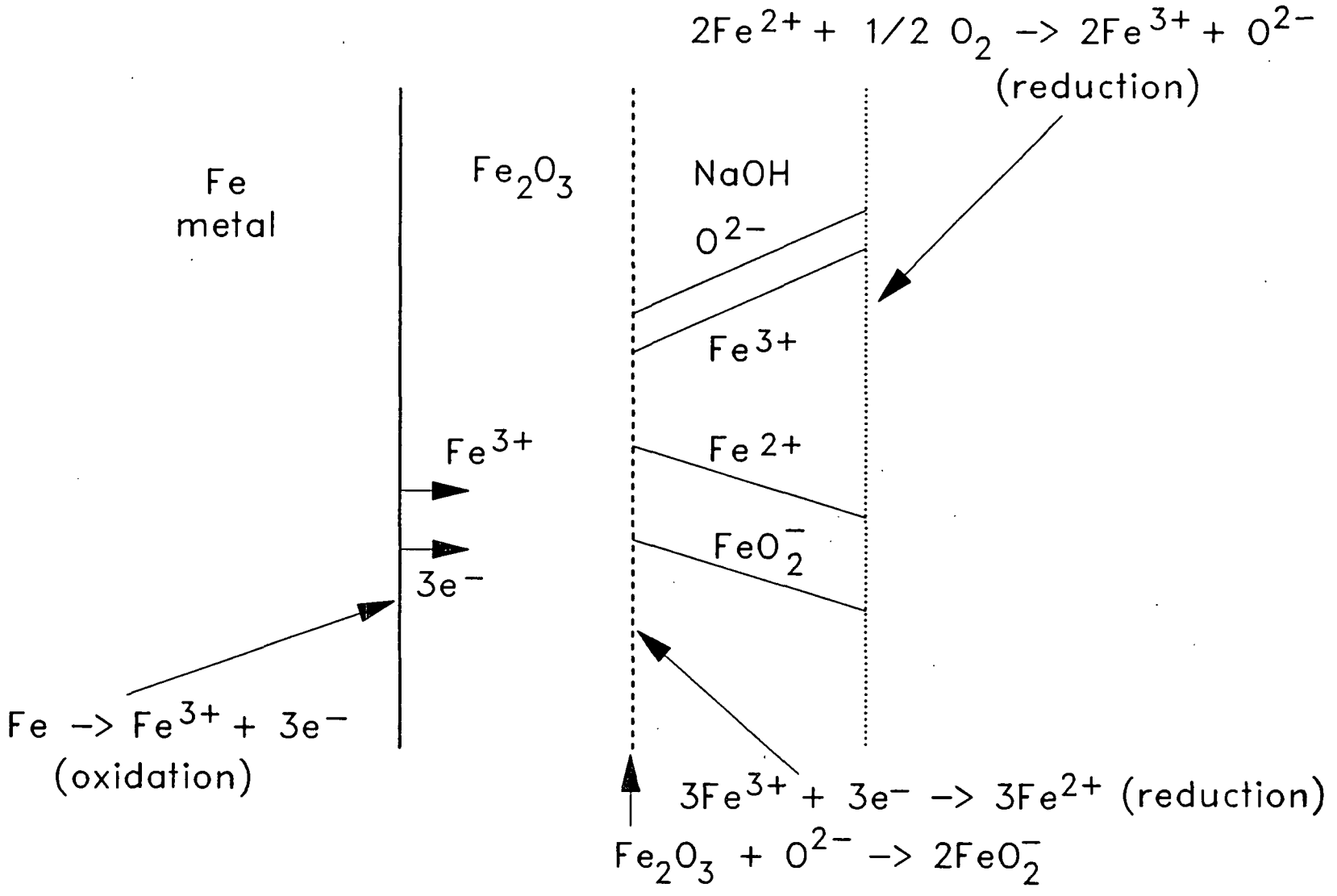

Figure 13. ***Electrochemical Model for Hot Corrosion of Fe in NaOH. Transition Metal Ion Transport Allows Reduction Reaction to Occur at Two Locations. Positive Solubility Gradient Would Limit Hot Corrosion.***